



PERGAMON

Solid State Communications 119 (2001) 377–380

solid  
state  
communications

www.elsevier.com/locate/ssc

# A new phase in polycrystalline magnetoresistive $\text{Sr}_2\text{FeMoO}_6$

M.X. Dai<sup>a,b,\*</sup>, C. Su<sup>a,b</sup>, R. Wang<sup>a,b</sup>, Z.L. Wang<sup>b,c</sup><sup>a</sup>Department of Physics, Wuhan University, 430072 Wuhan, People's Republic of China<sup>b</sup>Beijing Laboratory of Electron Microscopy, Chinese Academy of Sciences, 100080 Beijing, People's Republic of China<sup>c</sup>School of Materials Science and Engineering, Georgia Institute of Technology, Atlanta, GA 30332-0245, USA

Received 3 March 2001; received in revised form 21 May 2001; accepted 23 May 2001 by T.T.M. Palstra

## Abstract

A new layered body-centered tetragonal perovskite structure was observed in polycrystalline  $\text{Sr}_2\text{FeMoO}_6$  materials by transmission electron microscopy (TEM). Together with the double perovskite (DB) and the layered superstructure with tripled  $c$ -axis (ST) reported previously, the three ordered perovskite phases co-exists in the grain by sharing a common atomic plane of (001). The translation periodicity along the direction perpendicular to the layer plane is about 20 Å. © 2001 Elsevier Science Ltd. All rights reserved.

PACS: 75.30.Vn; 61.16.Bg; 61.66.Fn; 85.70.Kh

Keywords: C. Grain boundaries; C. Transmission electron microscopy; D. Tunneling

Practical applications of colossal magnetoresistive (CMR) oxides are limited by the large magnetic fields and/or low temperature required to observe a significant change in electric resistivity [1–5]. In recent years, research on tunneling magnetoresistance (TMR) is a very active field because of its scientific interest and potential technological applications [6]. Polycrystalline  $\text{Sr}_2\text{FeMoO}_6$  perovskite is a candidate for magnetic sensors owing to its high ferromagnetic transition temperature ( $T_c \sim 420$  K) and the half-metallic electronic band structure predicted theoretically [7]. The conduction electrons in this compound are expected to be highly spin-polarized even at room temperature. More recently, perovskite  $\text{Sr}_2\text{FeMoO}_6$  with nanometer grain size showed large magnetoresistance ( $\sim 20\%$ ) at a low magnetic field of 4 kOe and at room temperature [8]. Dai et al. [9] observed two different ordered structures in polycrystalline  $\text{Sr}_2\text{FeMoO}_6$  perovskite: the double perovskite and the superstructure with tripled  $c$ -axis (ST). In this paper, another new layered structure of body-centered tetragonal phase (BT) is reported for the polycrystalline magnetoresistive  $\text{Sr}_2\text{FeMoO}_6$  sample.

Ceramic samples of  $\text{Sr}_2\text{FeMoO}_6$  were prepared by

standard solid state reaction. Stoichiometric materials of  $\text{SrCO}_3$ ,  $\text{Fe}_2\text{O}_3$  and  $\text{MoO}_3$  were mechanically mixed, and then calcined at 950°C for 4 h in air. The calcined mixture was then ball-milled and made into pellets followed by sintering at 1250°C for 4 h in carbon monoxide atmosphere. Transmission electron microscopy (TEM) specimens were prepared by mechanical polishing, dimpling and ion milling. Electron diffraction patterns were taken at 120 kV using a Phillips CM12 electron microscope, and high resolution TEM imaging was conducted using JEOL 2010 microscope. Energy dispersion of X-rays (EDX) was conducted by TEM attached with EDAX PV9100.

By using a four-probe technique, the magnetoresistance (MR) for ceramic samples was measured to be about  $-5\%$  when a field of 2000 Oe was applied at room temperature. Fig. 1(a) shows a typical TEM image of  $\text{Sr}_2\text{FeMoO}_6$  sample. Selected area electron diffraction (SAED) revealed that it mainly consists of three phases relating to perovskite: double perovskite (DB) in area A, layered superstructure with tripled  $c$ -axis (ST) in area B, and a new layered structure of body-centered tetragonal phase (BT) in area C. Fig. 1(b) shows a high resolution TEM image of the new BT phase, showing layered structure. Fig. 2 shows electron diffraction patterns taken from area C in Fig. 1(a) oriented along [100], [110], [10 5 1] and [551], which correspond to [100], [110], [211] and [111] in the cubic system, respectively. For comparison with diffraction patterns of the

\* Corresponding author. Address: Department of Physics, Wuhan University, 430072 Wuhan, People's Republic of China. Fax: +86-27-87654569.

E-mail address: mx dai@whu.edu.cn (M.X. Dai).

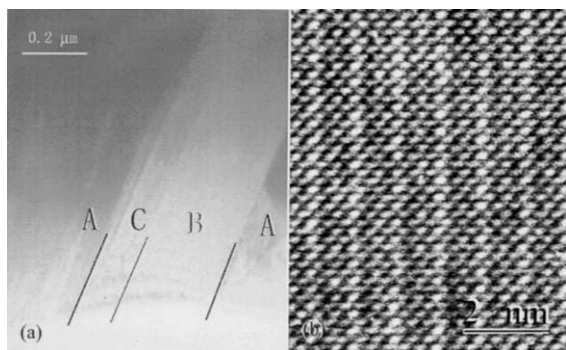


Fig. 1. (a) TEM image showing inter-phase boundaries in a  $\text{Sr}_2\text{FeMoO}_6$  grain. There are three phases corresponding to A, B and C areas. (b) High resolution electron microscopic image of a BT phase. The translation period along  $c$ -axis is about 20 Å in area C.

double perovskite phase (DP) reported previously (Dai et al., submitted), we choose the four main zone axes in the orientational triangle of the cubic phase, although it is not a cubic phase in Fig. 2. This is a new crystalline phase in the  $\text{Sr}_2\text{FeMoO}_6$  material. By careful examination of the extinction rules of electron diffraction, this new phase was verified to be a body-centered tetragonal phase (BT) with  $a \approx a_p$ ,  $b \approx a_p$  and  $c \approx 5a_p$ , where  $a_p$  is a translation period of a simple perovskite.

In order to reveal the relation among phases in the  $\text{Sr}_2\text{FeMoO}_6$  ceramics, the phase boundaries were examined by electron microscopy. Fig. 3(b) shows a planar phase boundary which separates area C from area A. Electron

diffraction experiment showed that it is a DP phase (in area A) and a BT phase (in area C). Fig. 3(a) and (c) shows electron diffraction patterns taken along a common direction (100) of two phases located in areas A and C, respectively. It can be seen that there are four weak diffraction spots between two strong spots along (0 0 10) diffraction series in Fig. 3(c). The reflection spot (002) in Fig. 3(a) is the basic reflection in the simple perovskite with a translation period of about 4 Å; the corresponding diffraction spot disappears in Fig. 3(c) because of the extinction rules for body centered tetragonal symmetry. From the high resolution electron microscopic image shown in Fig. 1(b), it can be seen that the translation period perpendicular to the layer plane is about 20 Å, which coincides with the super reflection series (0 0 10) in Fig. 3(c). Therefore, the lattice parameters of the unit cell in the BT phase are  $a \approx a_p$ ,  $b \approx a_p$  and  $c \approx 5a_p$ . Further experiments show that the phase boundary showing edge-on in Fig. 3(b) is parallel to the (001) plane in the two phases. In other words, the two grains (two phases) share a common (001) atomic plane. When the specimen was tilted while keeping the co-plane edge-on, another group of diffraction patterns were obtained. Fig. 3(e) and (f) shows EDPs along the [110] direction, taken from areas A and C, respectively. By inspecting the microscopic image of the grains with the incident electron beam parallel to this direction, the phase boundary plane is also edge-on (not shown in the figure). Further experiment evidenced that although the EDPs along [211] and [111] axes (in cubic index system) can be obtained by tilting the specimen in TEM, the edge-on condition of the phase boundary cannot be preserved.

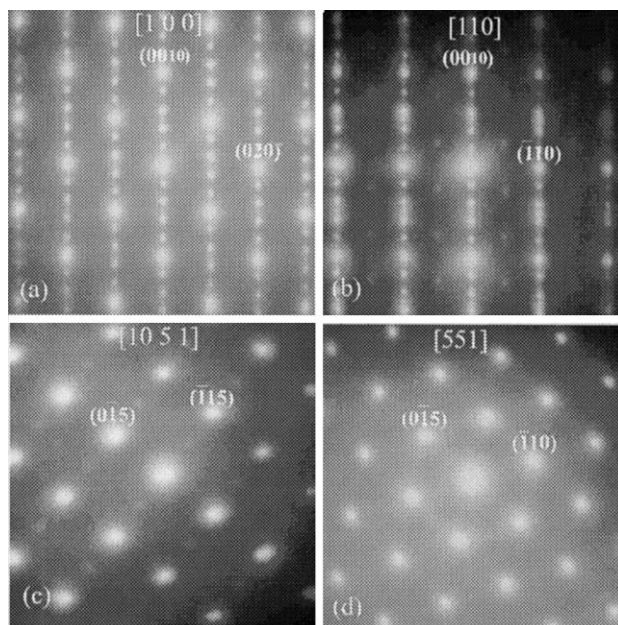


Fig. 2. Electron diffraction patterns from the body-centered tetragonal phase. The zone axes are [100], [110], [10 5 1] and [551] in (a), (b), (c) and (d), respectively, which correspond to the [100], [110], [211] and [111] zones in the cubic system.

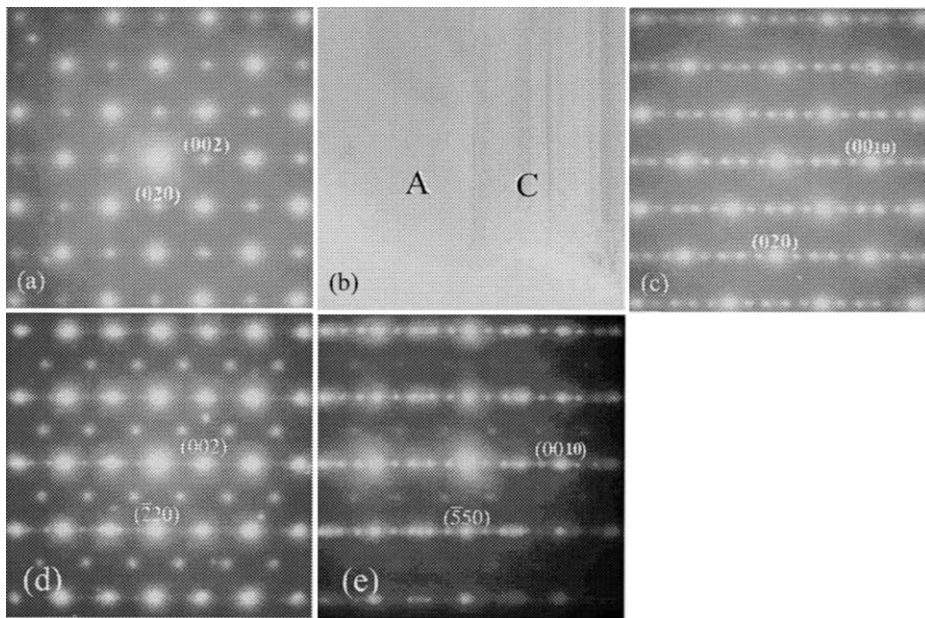


Fig. 3. (a) and (c) show electron diffraction patterns along [100] direction recorded from the areas A and B, respectively. (d) and (e) show the [110] electron diffraction patterns. (b) An edge-on inter-phase plane.

Fig. 4(b) shows another kind of phase boundary between the two different super structures whose common plane is (001). Fig. 4(a) and (c) shows the corresponding EDPs along [100] recorded, as the electron probe moves from the left to the right of the phase boundary, respectively. Trace analysis

shows that the super reflection spots in the two phases are along lines perpendicular to the phase boundary plane. The diffraction pattern in Fig. 4(c) shows four weak spots between the two strong spots, the same as those in Fig. 3(c), hence it is also the BT phase. However, five weak

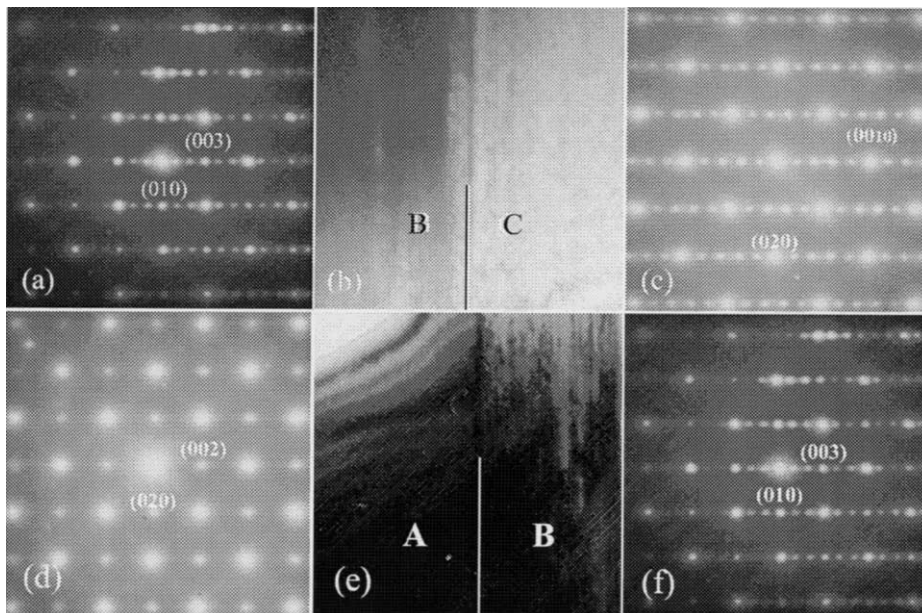


Fig. 4. Other two kinds of inter-phase planes. The second phase boundary plane between ST and BT phases in (b). (a) and (c) show electron diffraction patterns along [100] recorded from areas B and C, respectively. (d), (e) and (f) show the third phase boundary plane between DP and ST phases.

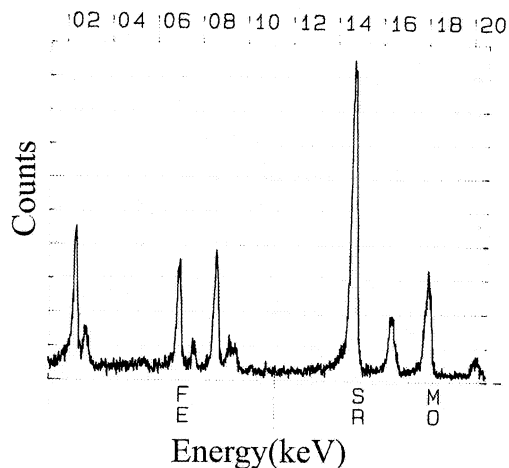


Fig. 5. EDX spectrum taken from BT phase in area C of Fig. 4(b).

spots can be seen between the two strong spots in the EDP displayed in Fig. 4(a). This phase is a layered perovskite with lattice parameters:  $a \approx a_p$ ,  $b \approx a_p$  and  $c \approx 3a_p$ , which was reported previously (Dai et al., submitted). Further experiment shows that the inter-phase plane is also edge-on as long as the incident electron beam is kept parallel to the common plane (001) when the specimen is tilted. If the incident beam deviates from the (001) atomic plane, the edge-on condition of the inter-phase plane cannot be preserved. Therefore, the inter-phase plane of the two phases is also parallel to (001).

There exists a third kind of phase boundary. Electron microscopy shows that the co-planar phase boundary is edge-on in Fig. 4(e) and is parallel to the (001) plane of the two phases. The left-hand part is the double perovskite (DP) and the right-hand part is the body-centered tetragonal phase (BT), as revealed by the EDPs along [100] axis in Fig. 4(d) and (f), respectively. Similarly the inter-phase plane (001) was verified from the electron diffraction experiment by the tilting of the specimen.

Fig. 5 shows an EDX spectrum taken from BT phase in area C of Fig. 4(b). The compositions were obtained by using a standard sample with correction of absorption. The elements, counts of X-rays and compositions are listed in Table 1. Besides the characteristic energy peaks of Fe, Sr and Mo, the characteristic energy peak of Cu is also appearing in Fig. 5, which is originated from specimen holder.

The newly observed body-centered tetragonal structure in  $\text{Sr}_2\text{FeMoO}_6$  is based on perovskite. A similar structure was previously discussed in  $\text{SrO-SrTiO}_3$  system [10]. In the present situation, the Ti sites were replaced by Fe and Mo

Table 1

Elements, counts per second (CPS) and atom percentages (at%) corresponding to area shown in Fig. 5

Elements	CPS	at%
Sr	85.229	25.0
Fe	24.110	9.2
Mo	27.050	9.0

at the centers of the oxygen octahedra, and this body-centered tetragonal structure is probably formed in the SrO-rich local areas. This is consistent with our EDX experimental result shown in Table 1. In general, magnetoresistance in polycrystalline ceramics is mainly a tunneling effect related to grain boundaries and inter-phase boundaries. Undoubtedly the existence of different crystalline phases with layered structures and inter-phase boundaries in ceramic samples are likely to affect the magnetoresistance of the material.

#### Acknowledgements

This work is supported by Trans-Century Programme Foundation for the Talents by the State Education Commission and National Natural Science Foundation of China (5982550).

#### References

- [1] M.N. Baibich, J.M. Broto, A. Fert, F.N.V. Dau, F. Petroff, P. Etienne, G. Creutzet, A. Fiefferich, J. Chazellas, *Phys. Rev. Lett.* 61 (1998) 2472.
- [2] R.V. Helmolt, J. Weckerg, B. Holzapfel, L. Schultz, K. Samwer, *Phys. Rev. Lett.* 71 (1993) 2331.
- [3] Z.L. Wang, J. Zhang, *Phys. Rev. B* 54 (1996) 1153.
- [4] Z.L. Wang, J.S. Yin, *Phil. Mag. B* 77 (1998) 49.
- [5] Z.L. Wang, Z.C. Kang, *Functional and Smart Material — Structural Evolution and Structure Analysis*, Plenum, New York, 1998.
- [6] J.S. Sun, W.J. Gallagher, P.R. Duncombe, L. Krusin-Elbaum, R.A. Tman, A. Gupta, Y. Lu, G.O. Gong, G. Xiao, *Appl. Phys. Lett.* 69 (1996) 3266.
- [7] K.-I. Kobayashi, T. Kimura, H. Sawada, K. Terakura, Y. Tokura, *Nature* 395 (1998) 677.
- [8] C.L. Yuan, S.G. Wang, W.H. Song, T. Yu, J.M. Dai, S.L. Ye, Y.P. Sun, *Appl. Phys. Lett.* 75 (1999) 3853.
- [9] M.X. Dai, C. Su, R. Wang, Z.L. Wang, submitted for publication.
- [10] M.A. McCoy, R.W. Grimes, W.E. Lee, *Phil. Mag. A* 75 (1997) 833.